

Universal structural softening in metallic glasses indicated by boson heat capacity peak

M. Q. Jiang, M. Peterlechner, Y. J. Wang, W. H. Wang, F. Jiang, L. H. Dai, and G. Wilde

Citation: *Appl. Phys. Lett.* **111**, 261901 (2017);

View online: <https://doi.org/10.1063/1.5016984>

View Table of Contents: <http://aip.scitation.org/toc/apl/111/26>

Published by the [American Institute of Physics](#)



SciLight

Sharp, quick summaries **illuminating**
the latest physics research

Sign up for **FREE!**

AIP
Publishing

Universal structural softening in metallic glasses indicated by boson heat capacity peak

M. Q. Jiang,^{1,2,3,a)} M. Peterlechner,² Y. J. Wang,^{1,3} W. H. Wang,⁴ F. Jiang,⁵ L. H. Dai,^{1,3} and G. Wilde^{2,6}

¹State Key Laboratory of Nonlinear Mechanics, Institute of Mechanics, Chinese Academy of Sciences, Beijing 100190, People's Republic of China

²Institute of Materials Physics, Westfälische Wilhelms-Universität Münster, Münster 48149, Germany

³School of Engineering Science, University of Chinese Academy of Sciences, Beijing 100049, People's Republic of China

⁴Institute of Physics, Chinese Academy of Sciences, Beijing 100190, People's Republic of China

⁵State Key Laboratory for Mechanical Behavior of Materials, Xi'an Jiaotong University, Xi'an 710049, People's Republic of China

⁶Herbert Gleiter Institute of Nanoscience, Nanjing University of Science and Technology, Nanjing 210094, People's Republic of China

(Received 22 November 2017; accepted 8 December 2017; published online 26 December 2017)

Low-temperature heat capacity is systematically investigated in various glassy and crystalline polymorphs of a wide range of metallic glasses. We reveal that the boson heat capacity peak beyond the Debye level arises from both excess phonon scattering and background electronic excitation, and the two contributions are strongly coupled and also material-dependent. It is interesting to observe that the boson heat capacity peaks obey an inversely linear correlation between their heights and characteristic positions, which is mainly dominated by phonic anomalies. This indicates a universal structural softening among the studied glasses when the boson peak occurs. We further suggest a possibility that the linear evolution of the fast boson peaks can probe into the slow structural softening across the glass transition, and the two dynamic processes are controlled by the short-time shear modulus associated with local soft regions in fragile glasses. *Published by AIP Publishing.* <https://doi.org/10.1063/1.5016984>

The nature of vibrations in glasses belongs to the grand mysteries in condensed matter physics. At terahertz (THz) frequencies, glasses generally exhibit an anomaly in their vibrational spectrum, i.e., the vibrational density of states (VDOSs) exceeds over the Debye level determined by continuum mechanics. This enhancement of THz excitations in glasses is called the “boson peak (BP)”. It is commonly believed that the BP pertains to all glasses,¹ irrespective of the bond types or the compositions and thus also including metallic glasses.² Despite much controversy, it now seems accepted that the BP originates from transverse phonons mixed with localized soft modes.^{3–5} The extra scattering of quasilocalized phonons contributes to an excess in the low-temperature T heat capacity C_p as compared to the Debye T^3 law. Thus, the excess heat capacity occurs visibly as a peak (namely, the “boson heat capacity peak”)^{6–9} in the plot of C_p/T^3 vs T at temperatures of ~ 10 K for all glasses.

Although it has not yet been completely understood,¹⁰ the BP opens a window into probing the intrinsic structural heterogeneity that plays a crucial role in glass relaxation and flow. Some intriguing correlations have been discovered between fast BP excitations and slow structural dynamics in glasses. For example, Sokolov *et al.*¹¹ found that the BP intensity increases with a decrease in the kinetic fragility. Experiments show that either mechanical deformation or isothermal aging can induce the evolution of the BP height and position.^{6,7,9,12} Recent simulations^{13–15} clearly demonstrate that quasilocalized soft modes (contributing to BPs) correlate

strongly with fertile regions for irreversible rearrangements or shear transformations.

Regardless of the specific reasons, the BP evolution itself exhibits a common feature:^{16–18} the stronger BPs always shift to lower frequencies/temperatures and vice versa. The universality of this behavior implies that the underlying origin of BPs may be quite fundamental in glasses albeit the diversity of microscopic constituents. Due to the structural simplicity and similarity, metallic glasses offer ideal model systems for exploring the evolution of the BPs. For metallic glasses, however, it is more complex to experimentally define the BP as a peak in C_p/T^3 vs T . This is because the electronic heat capacity inevitably interferes at such low temperatures. At least the boson heat capacity peak has to include quasilocalized phonic and background electronic contributions, and sometimes, the latter could hide the former, due to a strong electron-phonon coupling. Naturally, one would like to ask how the boson heat capacity peak evolves in metallic glasses with the inherent interaction of electrons and phonons, which is not covered previously.

In this Letter, we report a systematic study on the boson heat capacity peaks of various glassy and crystalline polymorphs of a wide range of metallic glasses. By examining the Sommerfeld coefficient γ , it is demonstrated that the electronic contribution to C_p is extremely sensitive to the topological and chemical disorder of glasses. The significant electronic contribution will hide the BPs in C_p/T^3 -plots, causing an apparent anomaly of their evolution. By subtracting the electronic part from the low-temperature C_p , we can locate the boson peak whose evolution still exhibits the common

^{a)} Author to whom correspondence should be addressed: mqjiang@imech.ac.cn

feature. More importantly, it is revealed that the heights of the boson heat capacity peaks follow an inversely linear relationship with temperature at which C_p/T^3 is maximum. This implies a universal structural softening in metallic glasses when the BP occurs. The BP-indicated softening shows a possible link to the structural softening across the glass transition, and both dynamic processes are shear-dominated on short timescales.^{3,19}

Vitreloy 1, with a nominal composition of $\text{Zr}_{41.2}\text{Ti}_{13.8}\text{Cu}_{12.5}\text{Ni}_{10}\text{Be}_{22.5}$ (at. %), was chosen as a model metallic glass to show the evolution of boson heat capacity peaks in different topological states. The low-temperature ($1.9\text{ K} \leq T \leq 100\text{ K}$) specific heat capacity C_p was measured using a Quantum Design physical property measurement system (PPMS) on the as-cast glassy, annealed glassy, and fully polycrystalline states of the Vitreloy 1. The [supplementary material](#) describes how the three Vitreloy 1 states have been synthesized and characterized.

Figure 1(a) plots the specific heat capacity C_p for the as-cast, annealed, and crystallized Vitreloy 1 in the temperature interval of 1.9–100 K. The inset shows the corresponding log-log plot. As expected, the heat capacity C_p for each state decreases with decreasing temperature. All C_p data will approach zero if $T \rightarrow 0\text{ K}$, and their high-temperature limit is about $0.416\text{ J g}^{-1}\text{ K}^{-1}$, determined by the Dulong-Petit

law. The heat treatment reduces the heat capacity by deepening inherent structures (ISs) of glasses.^{20,21} Figure 1(b) plots the specific heat capacity data as C_p/T^3 vs T to reveal the BPs beyond the Debye level. In this plot, the ordering-induced decrease of C_p becomes more apparent. For the as-cast and annealed Vitreloy 1 glasses, the BP only appears as an obscure shoulder and cannot be readily identified. However, the Vitreloy 1 polycrystal exhibits a visible BP-like anomaly at about 20 K. This kind of anomaly has been previously observed in crystalline materials,^{7,22,23} always showing a significantly higher peak temperature/frequency compared to that of the glass BPs. We believe that the currently observed C_p anomaly stems from disordered lattices at nanograin boundaries that abound in the polycrystalline alloys (see [supplementary material](#) Fig. S3). The underlying mechanism is the transverse acoustic (TA) van Hove singularity,^{17,23} a suggested counterpart of the glass BPs in crystals. A question thus arises why the Vitreloy 1 glass with a higher degree of disorder does not show a pronounced BP? According to the seminal study of Li *et al.*,²⁴ such a paradox is attributed to the contribution of electronic excitations to low-temperature C_p . The electronic C_p is typical of metallic glasses or crystalline alloys but does not exist in traditional glasses without metallic bonding. It is thus speculate that the electronic C_p might be relatively weak in the alloys with higher structural order. In other words, the electronic C_p contribution should highly depend on the topological disorder/order in alloys.

We determine the electronic C_p contribution by plotting C_p/T vs T^2 below 8 K for the as-cast, annealed, and crystallized Vitreloy 1 (see [supplementary material](#) Fig. S4). The low-temperature C_p data can be well fitted with the formula $C_p/T = \beta T^2 + \gamma$, where the Sommerfeld coefficient γ measures the degree of electronic contribution. It is worth noting that γ becomes smaller for the heavily heat treated Vitreloy 1. For the annealed states, γ decreases by about 3% as compared with that of the as-cast, and γ of the crystallized states decreases by about 33%. This behavior implies a strong electron-phonon coupling that contributes to the low-temperature C_p in glassy or crystalline states of the alloy. The electronic C_p contribution becomes more significant in highly disordered alloys. Contrarily, topological/structural ordering induced by heat treatment decreases the electronic contribution γ , making the boson heat capacity peaks more visible. This explains why the polycrystalline Vitreloy 1 exhibits a pronounced “BP” that is a multiplex consequence of the plentiful disordered boundaries (TA singularity) and relatively weak electronic contribution to C_p .

Our analysis confirms that the boson heat capacity peaks due to phonic anomalies can be determined by subtracting the linear electronic contribution γT . Actually, this approach has been widely adopted in metallic glasses.^{6,8,24,25} An alternative approach defines a boson peak as the difference between C_p/T^3 of the glass and the corresponding crystal. However, it is very difficult to find such a reference crystal that does not show a BP-like C_p anomaly and meanwhile has the same electronic C_p as that of the glass. Here, we adopt the first approach because we believe that it reflects the essential properties of BPs.

Figure 2 plots the specific heat capacity as C_p/T^3 and $(C_p - \gamma T)/T^3$ vs T for the as-cast, annealed, and crystallized

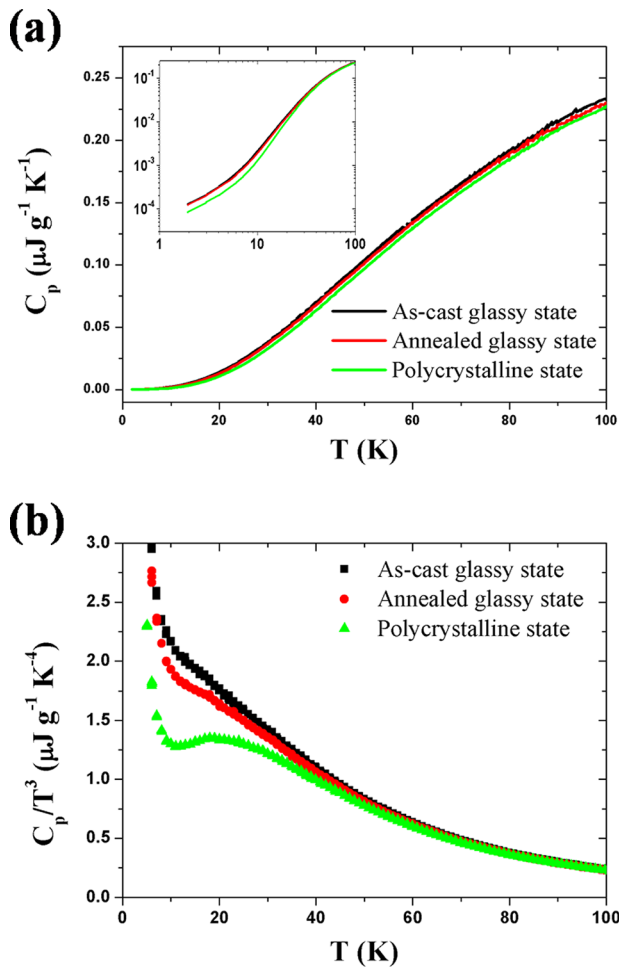


FIG. 1. Low-temperature (a) C_p and (b) C_p/T^3 vs T plot for the as-cast, annealed, and crystallized Vitreloy 1. Inset in (a): the corresponding log-log plot.

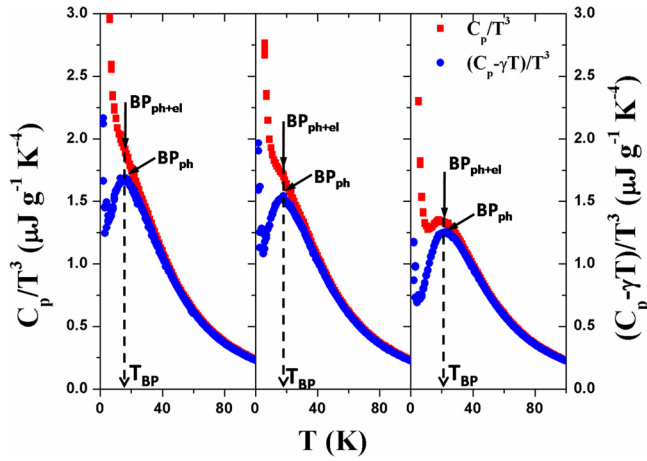


FIG. 2. Low-temperature C_p/T^3 and $(C_p - \gamma T)/T^3$ vs T for the as-cast, annealed, and crystallized Vitreloy 1 (from left to right).

Vitreloy 1 (from left to right). As compared with C_p/T^3 , the $(C_p - \gamma T)/T^3$ curves clearly show where the BPs take place, and the position temperatures T_{BP} of the BPs are readily located. More importantly, we obtain two kinds of boson heat capacity peaks. One as a peak in the $(C_p - \gamma T)/T^3$ plot is only due to the atomic vibrational or phonic anomaly, denoted as BP_{ph} . The other involves the electronic contribution γT_{BP} in addition to the phonic BP_{ph} , denoted as BP_{ph+el} in the C_p/T^3 plot. The heights corresponding to BP_{ph} and BP_{ph+el} can be determined, respectively, as

$$H_{ph} = \left(\frac{C_p - \gamma T}{T^3} \right)_{T_{BP}}, \quad (1)$$

$$H_{ph+el} = \left(\frac{C_p}{T^3} \right)_{T_{BP}}. \quad (2)$$

For Vitreloy 1, the evolution of both BP_{ph} and BP_{ph+el} induced by structural changes still follows the common feature. The stronger (higher H_{ph} or H_{ph+el}) the boson heat capacity peaks are the lower the corresponding temperatures (T_{BP}) are observed. The as-cast Vitreloy 1 glass that corresponds to the state of the highest disorder shows the strongest BPs where both phonic and electronic contributions are highest. The polycrystalline Vitreloy 1 shows the lowest “BPs” with the weakest phonic and electronic contributions. The BP of the annealed glassy Vitreloy 1 takes an intermediate level.

The universality of evolution of boson heat capacity peaks has been further studied in more systems or states of metallic glasses, in addition to the above three states of Vitreloy 1. Additional 10 PPMS- C_p measurements were performed on Vitreloy 1 (quenched), $Zr_{52.5}Cu_{17.9}Ni_{14.6}Al_{10}Ti_5$, $Zr_{50}Cu_{40}Al_{10}$, $Zr_{55}Cu_{30}Al_{10}Ni_5$, $Pd_{40}Ni_{40}P_{20}$, and $Zr_{64.13}Cu_{15.75}Ni_{10.12}Al_{10}$ in the temperature range of 1.9–100 K. Their BP positions T_{BP} and heights (H_{ph} and H_{ph+el}), as well as the Sommerfeld coefficients γ , were determined (see [supplementary material Table S1](#)) according to the aforementioned approach. Table S1 ([supplementary material](#)) also lists the relevant data of other 28 metallic glasses, including Zr-, Pd-, and Cu-based, that can be found or calculated from the recent literature.^{6,7,25–28} Since for some glasses, γ cannot be determined, 33 datasets are available in total for H_{ph} and 41 datasets for H_{ph+el} .

Figure 3(a) presents the phonic BP_{ph} evolution among various metallic glasses by plotting their H_{ph} vs $1/T_{BP}$. Obviously, stronger BP_{ph} with higher H_{ph} corresponds to lower T_{BP} and vice versa. Disordered glasses formed by fast cooling move to the upper right corner of Fig. 3(a), while those well annealed reside in the lower left corner, as well as their crystallized states. There appears to be a general linear trend between H_{ph} and T_{BP} ; however, the data are noted to a little bit scatter. We believe that this scatter results from the inherent effect of the additional electronic C_p contribution. It is indeed found that the Sommerfeld coefficients γ are extremely sensitive to glassy structures and compositions (see [supplementary material Table S1](#)). Such a strong electron-phonon coupling leads to the material-dependent contribution to BP from either phonons or electrons. Quite interestingly, when we plot H_{ph+el} vs $1/T_{BP}$, as shown in Fig. 3(b), all data collapse well onto a single master straight line. This indicates that the combination of the two material-dependent contributions does not depend on specific glasses any longer. The observed linear correlation can be well fitted by

$$H_{ph+el} = \left(\frac{C_p}{T^3} \right)_{T_{BP}} = \Gamma \frac{1}{T_{BP}} + \Phi, \quad (3)$$

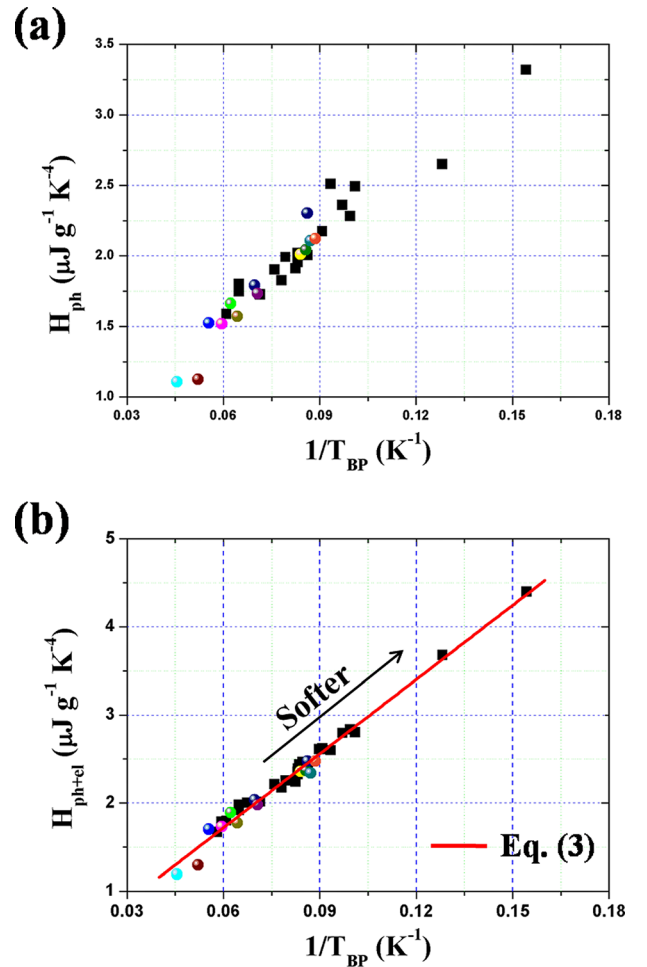


FIG. 3. Evolution of boson capacity heat peaks in metallic glasses by plotting their heights (a) H_{ph} and (b) H_{ph+el} as a function of positions $1/T_{BP}$. The solid line in (b) is the least-squares fitting by Eq. (3). Colorful spheres: data in this work; black squares: data from the literature.

where the universal slope ($\Gamma = 28.58$) implies the existence of a fundamental behavior of various glassy structures. The intercept ($\Phi = 0.014$) is supposed to be less meaningful since it is much less than $H_{\text{ph+el}}$ by at least 2 orders of magnitude.

Figure 3 clearly demonstrates that, although it is improved by the electronic contribution, the observed linear correlation (3) is mainly dominated by the extra atomic vibrations. In what follows, we only consider the dominated phonic effect that is actually coupled with the secondary electronic contribution. Therefore, this implies that the VDOS BPs of glasses in general may also show a linear evolution between their heights and characteristic frequencies, which has been supported by simulations^{3,29} and experiments.^{17,30} For example, Grigera *et al.*²⁹ computed the VDOS $g(\omega)$ of the IS of a fragile glass using the Swap Monte Carlo algorithm. By changing the temperatures, they found that the height $g(\omega_{\text{BP}})/\omega_{\text{BP}}^2$ and the position ω_{BP} of the BPs satisfy a scaling law, which is only controlled by the IS energy. At temperatures well below the mode-coupling temperature, this scaling law approximates to an inversely linear behavior (or linear if adopting $1/\omega_{\text{BP}}$ like $1/T_{\text{BP}}$ here). Recently, using nuclear inelastic scattering, Chumakov *et al.*¹⁷ measured the iron-partial VDOS of a sodium silicate glass at various pressures. The phenomenon that the shift of BPs is nearly linear between their heights and positions can also be noted. In the present work, of great interest is that the different boson heat capacity peaks of various metallic glasses display an identical linear evolution. Such a universal behavior implies that the characteristic structures responsible for BPs are of, to some extent, similarity or resemblance for the studied glasses.

As already discussed, the BP *per se* arises from quasilo-calized soft modes, i.e., transverse vibrational modes associated with local soft regions (LSRs).^{3,13,14} The long-range elastic correlations of these LSRs cause a strong excess phonon scattering³¹ so that transverse acoustic phonons eventually lose their wave-like character, appearing as the BP. We note that the metallic glasses listed in [supplementary material Table S1](#) belong to fragile liquids. In these glasses, LSRs construct a majority matrix phase surrounding strongly bonded regions. Therefore, the global shear modulus of glasses is mainly controlled by the local shear modulus of these LSRs, obeying the mechanical series model.^{32,33} In this scenario, Shintani and Tanaka³ suggested that the BP height is inversely proportional to the shear modulus. Vasiliev *et al.*²² further validated this simple relation and found that it is indeed controlled by the defect concentration akin to the fraction of LSRs. By the same token, we reasonably assume that

$$H_{\text{ph+el}} = \left(\frac{C_p}{T^3} \right)_{T_{\text{BP}}} \propto \frac{1}{G_\infty}, \quad (4)$$

where G_∞ is the instantaneous shear modulus of glasses due to the extremely low-temperature (~ 10 K) or high-frequency (THz) condition. Upon substituting Eq. (4) into Eq. (3), we get the expression of the slope Γ

$$\Gamma = \frac{1}{dG_\infty/dT_{\text{BP}}}. \quad (5)$$

It reveals that $1/\Gamma$ corresponds to the linear change of G_∞ among various metallic glasses (T_{BP}), that is, $dG_\infty/dT_{\text{BP}} \approx 0.035$ GPa/K; here, all dimension anharmonicities are observed in Eq. (4). This linear G_∞ -change actually reflects a universal sample-to-sample structural softening, which can be precisely probed by the shift of the boson capacity heat peaks.

In glass science, an idea that the instantaneous shear modulus G_∞ can determine the glass flow is gaining increasing support from experiments,³⁴ simulations³⁵ to theories.^{19,36} A typical G_∞ -governed flow is the glass transition upon heating. As illustrated in Fig. 4, the glass transition can be represented as the α -relaxation hopping from a “metabasin” to a neighboring relatively shallower one in ISs of the potential energy landscape (PEL). Such a hopping event is essentially indistinguishable in the perspective of the static structures but can be detected by the decrease in G_∞ that is the second derivation of the PEL of “metabasin”. As discussed above, the change of G_∞ closely links with the evolution of BPs. It is therefore tempting to relate the G_∞ -governed softening at T_{BP} to that at the glass transition temperature T_g , leading to

$$\Gamma = \frac{1}{dG_\infty/dT_{\text{BP}}} \approx \frac{1}{|dG_\infty/dT|_{T_g}}. \quad (6)$$

To prove this speculation, data on $|dG_\infty/dT|_{T_g}$ are required. It is very difficult to precisely measure the instantaneous shear modulus G_∞ of a frozen IS structure that undergoes the glass transition. Nevertheless, we identified three reports on experimental work, where the ultrasonic method was adopted to approximately frozen glass configurations. Lind *et al.*³⁷ found that for the Vitreloy 4 ($\text{Zr}_{46.75}\text{Ti}_{8.25}\text{Cu}_{7.5}\text{Ni}_{10}\text{Be}_{27.5}$) having different configurational states, their equilibrium liquid shows a strong linear relation $|dG_\infty/dT|_{T_g} = 0.035$ GPa/K around T_g . Keryvin *et al.*³⁸ measured the change in Young’s modulus E_∞ during a linear heating for a $\text{Zr}_{55}\text{Cu}_{30}\text{Ni}_{15}\text{Al}_{10}$ metallic glass. They found that there is a fast softening rate, $|dE_\infty/dT|_{T_g} = 0.089$ GPa/K, at T_g . For metallic glasses, $G/E = 0.39$ is well satisfied.³⁹ This also leads to $|dG_\infty/dT|_{T_g} \approx 0.035$ GPa/K. Khonik *et al.*²⁷ performed direct *in situ*

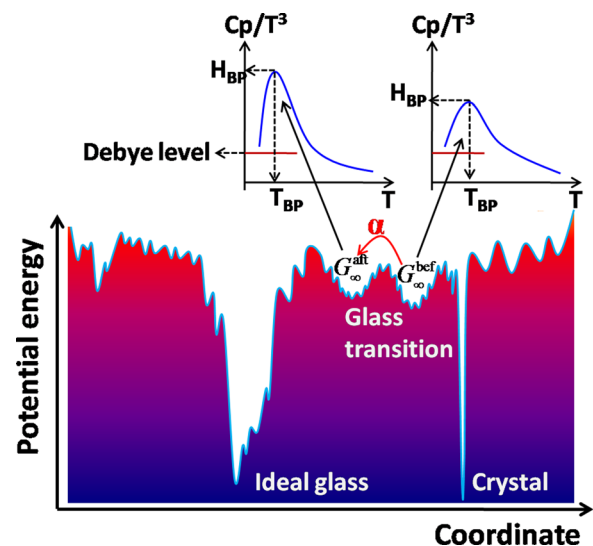


FIG. 4. A schematic illustration of the PEL showing a possible link between the boson-peak-change and the glass transition in glasses.

measurements of G_{∞} of the as-cast and annealed bulk $\text{Pd}_{40}\text{Cu}_{30}\text{Ni}_{10}\text{P}_{20}$ below and above T_g . A linear relation $|dG_{\infty}/dT|_{T_g} \approx 0.034 \text{ GPa/K}$ was again observed. Such a striking agreement indicates a possibility that the THz BP anomaly and the glass transition on long timescales share the identical dynamic or even structural origin. Our results demonstrate that the sample-to-sample structural softening when the BP occurs is physically akin to the sample's hopping on different "metabasins" in the ISs across the glass transition (see Fig. 4).

In conclusion, we systematically measured or analyzed the low-temperature heat capacity of various glassy and crystalline polymorphs of a wide range of metallic glasses. By distinguishing between the excess phonic scattering and background electronic excitation, we exactly locate the boson heat capacity peak. A main finding of the present study is that the boson heat capacity peaks involving both phonic and electronic contributions show an inversely linear correlation between their heights and position temperatures. The observed correlation implies a universal shear or structural softening among the studied metallic glasses, which can be understood in terms of transverse soft modes associated with local soft regions. We further bridge a possible link between the fast boson peak softening and the slow structural softening across the glass transition via the short-time shear modulus. Our work suggests that, mediated by G_{∞} , the BP can be adopted to probe the glass transition. It must be pointed out that the present findings may not be valid for metallic glasses with significant magnetic heat capacity, heavy-fermion behavior, or belonging to strong liquids. In addition, for metallic glasses, the quantitative phonon-electron interaction deserves further investigations for deepening our fundamental understanding of low-temperature calorimetry anomalies.

See [supplementary material](#) for the preparation, heat treatments, and structural characterization of the Vitreloy 1 as well as the analytical data about the low-temperature heat capacity for various metallic glasses and their crystalline counterparts.

This work was supported by the National Natural Science Foundation of China (Grant Nos. 11522221, 11790292, and 11372315), the Strategic Priority Research Program (Grant No. XDB22040303), and the Key Research Program of Frontier Sciences (Grant No. QYZDJSSW-JSC011) of the Chinese Academy of Sciences. G.W. acknowledges support by D.F.G. through Grant No. Wi 1899/27-2 as part of SPP1594.

¹L. Gil, M. A. Ramos, A. Bringer, and U. Buchenau, *Phys. Rev. Lett.* **70**, 182 (1993).

²T. Scopigno, J. B. Suck, R. Angelini, F. Albergamo, and G. Ruocco, *Phys. Rev. Lett.* **96**, 135501 (2006).

³H. Shintani and H. Tanaka, *Nat. Mater.* **7**, 870 (2008).

⁴H. R. Schober, *J. Non-Cryst. Solids* **357**, 501 (2011).

⁵P. M. Derlet, R. Maaß, and J. F. Löffler, *Eur. Phys. J. B* **85**, 148 (2012).

⁶B. Huang, H. Y. Bai, and W. H. Wang, *J. Appl. Phys.* **115**, 153505 (2014).

⁷Y. P. Mitrofanov, M. Peterlechner, S. V. Divinski, and G. Wilde, *Phys. Rev. Lett.* **112**, 135901 (2014).

⁸Y. P. Mitrofanov, M. Peterlechner, I. Binkowski, M. Y. Zadorozhnyy, I. S. Golovin, S. V. Divinski, and G. Wilde, *Acta Mater.* **90**, 318 (2015).

⁹P. Luo, Y. Z. Li, H. Y. Bai, P. Wen, and W. H. Wang, *Phys. Rev. Lett.* **116**, 175901 (2016).

¹⁰R. Zorn, *Physics* **4**, 44 (2011).

¹¹A. P. Sokolov, R. Calemczuk, B. Salce, A. Kisliuk, D. Quitmann, and E. Duval, *Phys. Rev. Lett.* **78**, 2405 (1997).

¹²J. Bünz, T. Brink, K. Tsuchiya, F. Meng, G. Wilde, and K. Albe, *Phys. Rev. Lett.* **112**, 135501 (2014).

¹³A. Widmer-Cooper, H. Perry, P. Harrowell, and D. R. Reichman, *Nat. Phys.* **4**, 711 (2008).

¹⁴M. L. Manning and A. J. Liu, *Phys. Rev. Lett.* **107**, 108302 (2011).

¹⁵J. Ding, S. Patinet, M. L. Falk, Y. Q. Cheng, and E. Ma, *Proc. Natl. Acad. Sci. U. S. A.* **111**, 14052 (2014).

¹⁶R. Zorn, *Phys. Rev. B* **81**, 054208 (2010).

¹⁷A. I. Chumakov, G. Monaco, A. Monaco, W. A. Crichton, A. Bosak, R. Ruffer, A. Meyer, F. Kargl, L. Comez, D. Fioretto *et al.*, *Phys. Rev. Lett.* **106**, 225501 (2011).

¹⁸A. I. Chumakov, G. Monaco, A. Fontana, A. Bosak, R. P. Hermann, D. Bessas, B. Wehinger, W. A. Crichton, M. Krisch, R. Rüffer *et al.*, *Phys. Rev. Lett.* **112**, 025502 (2014).

¹⁹J. C. Dyre and N. B. Olsen, *Phys. Rev. E* **69**, 042501 (2004).

²⁰F. Sciortino, *J. Stat. Mech. Theory Exp.* **2005**, P05015.

²¹M. Q. Jiang, M. Naderi, Y. J. Wang, M. Peterlechner, X. F. Liu, F. Zeng, F. Jiang, L. H. Dai, and G. Wilde, *AIP Adv.* **5**, 127133 (2015).

²²A. N. Vasiliev, T. N. Voloshok, A. V. Granato, D. M. Joncich, Y. P. Mitrofanov, and V. A. Khonik, *Phys. Rev. B* **80**, 172102 (2009).

²³A. Gupta, B. T. Kavakbasi, B. Dutta, B. Grabowski, M. Peterlechner, T. Hickel, S. V. Divinski, G. Wilde, and J. Neugebauer, *Phys. Rev. B* **95**, 094307 (2017).

²⁴Y. Li, P. Yu, and H. Y. Bai, *Appl. Phys. Lett.* **86**, 231909 (2005).

²⁵Y. Li, P. Yu, and H. Y. Bai, *J. Appl. Phys.* **104**, 013520 (2008).

²⁶Y. Tian, Z. Q. Li, and E. Y. Jiang, *Solid State Commun.* **149**, 1527 (2009).

²⁷V. A. Khonik, Y. P. Mitrofanov, S. A. Lyakhov, A. N. Vasiliev, S. V. Khonik, and D. A. Khoviv, *Phys. Rev. B* **79**, 132204 (2009).

²⁸W. M. Yang, H. S. Liu, X. J. Liu, G. X. Chen, C. C. Dun, Y. C. Zhao, Q. K. Man, C. T. Chang, B. L. Shen, A. Inoue *et al.*, *J. Appl. Phys.* **116**, 123512 (2014).

²⁹T. S. Grigera, V. Martin-Mayor, G. Parisi, and P. Verrocchio, *Nature* **422**, 289 (2003).

³⁰V. K. Malinovsky and A. P. Sokolov, *Solid State Commun.* **57**, 757 (1986).

³¹S. Gelin, H. Tanaka, and A. Lemaitre, *Nat. Mater.* **15**, 1177–1181 (2016).

³²D. Ma, A. D. Stoica, X. L. Wang, Z. P. Lu, B. Clausen, and D. W. Brown, *Phys. Rev. Lett.* **108**, 085501 (2012).

³³W. H. Wang, *Nat. Mater.* **11**, 275 (2012).

³⁴T. Scopigno, G. Ruocco, F. Sette, and G. Monaco, *Science* **302**, 849 (2003).

³⁵P. Bordat, F. Affouard, M. Descamps, and K. L. Ngai, *Phys. Rev. Lett.* **93**, 105502 (2004).

³⁶M. Q. Jiang and L. H. Dai, *Phys. Rev. B* **76**, 054204 (2007).

³⁷M. L. Lind, G. Duan, and W. L. Johnson, *Phys. Rev. Lett.* **97**, 015501 (2006).

³⁸Y. Keryvin, M. L. Vaillant, T. Rouxel, M. Huger, T. Gloriant, and Y. Kawamura, *Intermetallics* **10**, 1289 (2002).

³⁹M. Q. Jiang and L. H. Dai, *Philos. Mag. Lett.* **90**, 269 (2010).